

Complete Bilayer Adsorption Of C₁₆TAB On The Surface Of Mica Using Neutron Reflection

L. R. Griffin^a, K. L. Browning^a, C.L. Truscott^a, L. A. Clifton^b and S. M. Clarke^{a}*

^a BP Institute and Department of Chemistry, University of Cambridge, Cambridge, CB3 0EZ

^b ISIS, Rutherford Appleton Laboratory, Didcot, Oxfordshire, UK

In this work we present neutron reflection data from an alkylammonium surfactant (C₁₆TAB) at the mica/water interface. The system is studied in situ in a non-invasive manner and indicates the formation of a complete adsorbed bilayer with little evidence of defects. A detailed analysis suggests that the data is not consistent with some other previously reported adsorbed structures, such as micelles or cylinders.

Introduction

Understanding the behaviour of surfactants at the mica/water interface lies at the heart of a number of industrial processes such as flotation and detergency. In this context the adsorbed layer structures of industrially important surfactants have been the subject of a number of studies. In this work we address the adsorption of the cationic surfactant, hexadecyltrimethylammonium bromide – C₁₆TAB illustrated in Figure 1.

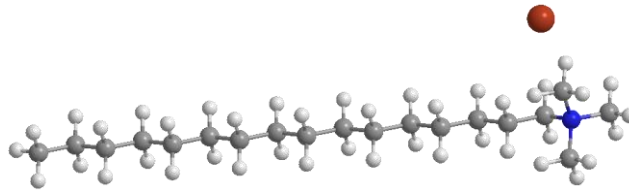


Figure 1 Molecular structure of C₁₆TAB obtained from ChemBio3D Ultra: Hydrogen in white, carbon in grey, nitrogen in blue, bromine in red.

Neutron reflection is a powerful tool for study of interfaces enabling buried interfaces to be studied non-invasively. The strength of this technique lies in its unique facility for contrast matching by isotopic exchange to enhance sensitivity to particular species of interest, often adsorbed organics. Hydrogen and deuterium have scattering length densities of opposite signs and so mixtures of deuterated and hydrogenated solvents or adsorbates enable multiple contrasts of structurally equivalent systems to be recorded. This enables fitting of a more constrained model resulting in improved structural characterisation. As such, neutron reflection has already been exploited to study the C_nTABs on silica¹⁻³ and quartz^{4,5}. These studies report bilayer like structures for CTAB even at low coverages.

Challenging substrate requirements for neutron reflection mean that this technique has not historically been applied to the mica surface. A high absorption cross section and scattering from defects in the mineral means neutron reflection from mica bulk is not possible. Cosgrove *et al* used an incident beam through a thin film of solvent which was always contrast matched to air to avoid contributions from the liquid/air interface to the reflected signal⁶. However, this approach did not achieve sufficient substrate flatness for the required reflected intensity. More recently, Browning *et al* showed that by supporting a thin layer of mica on a silicon substrate both flatness

and transmission problems can be circumvented and high quality neutron reflectivity data obtained from the mica/water interface⁷.

There are a number of reports of the adsorbed layer structure of the C₁₆TAB at the mica/water interface using SFA⁸⁻¹¹, AFM¹²⁻¹⁴ and XRR^{15,16}. A number of different surface aggregate structures (spheres¹², cylinders^{12,14}, bilayers^{8,15,16}) are reported using these different techniques.

Using AFM Liu *et al* report that below the Kraft temperature, C_{16,18,20}TAB all formed flat layers on mica at twice the CMC¹³. Estimates of the layer thicknesses are all less than twice the extended length of the molecule; a result consistent with some interdigitation or tilting of the surfactant tails in the layer¹³. AFM studies also report that adsorption of alkyltrimethylammonium bromides on mica below the Kraft temperature (25°C) is slow to reach equilibrium. C₁₆TAB is reported to initially adsorb as cylindrical aggregates which then undergo a structural evolution over a period of 6 to 24 hours where aggregates flatten into a bilayer^{8,12,14} and a second weakly attached bilayer is formed on top of the first¹¹.

Recent work by Speranza *et al* used their 'bending mica' technique to study the mica/water interface using x-ray reflectivity (XRR)^{15,16}. A series of C_nTABs (n=10,12,14,16 and 18) were reported to form tilted or interdigitated bilayers at concentrations ranging from 0.1 to 10 CMC where the surface coverage and thickness increased with the bulk surfactant concentration reaching a maximum at roughly 1 CMC.

With the exception of XRR, the techniques previously used to study the mica/water interface require the introduction of a second surface which may perturb the adsorbed layer structure. Significantly, adsorbed micellar structures were only observed using these invasive techniques suggesting that interference from the AFM probe may cause transient structures at the surface.

In this work we use contrast variation and non-invasive nature of neutron reflection to study C₁₆TAB adsorption at the mica/water interface.

Experimental Methods and Analysis

Materials

Mica substrates were prepared as described by Browning *et al*⁷. In this work the silicon blocks (Siltronix, France) used were 50 mm x 100 mm x 10 mm and covered with mica bound with a UV cured adhesive (Loctite 3301). A solid/liquid interface was created by clamping a Teflon trough to the mica with a slightly smaller size (40 mm x 85 mm) than the mica to avoid any imperfections at the edges of the mica.

Hexadecyltrimethylammonium bromide (Sigma Aldrich >99 %) was checked for purity using drop shape analysis; no minimum in the surface tension was detected before the CMC (measured as 1.0 mM in good agreement with literature values¹⁷) and used as received. All glassware and sample containers were cleaned in concentrated nitric acid for four hours and rinsed copiously with ultra-pure water (Millipore 18.2 MΩ cm⁻¹) and allowed to soak in water overnight before use.

Solutions of C₁₆TAB in D₂O and H₂O were made at 1 CMC (1.0 mM). Solutions were introduced to the neutron cell by HPLC pump (L7100 HPLC pump, Merck, Hitachi). A thorough exchange was ensured by pumping 14 times the cell volume (24 mL) at 2 mL min⁻¹ as determined by a previous study. The initial filling of the cells was carried out vertically with the liquid entering from the bottom of the cells at 5 mL min⁻¹ whilst rocking until no air bubbles were visible in the liquid out line.

Table 1 Fitted scattering length densities of materials used during this study. *Calculated from chemical formula $C_{41}H_{65}NO_{15}$ determined by elemental analysis of the glue studied and the cured glue density, 1.16 g cm^{-3} (from Loctite 3301® Technical Data Sheet)

Material	SLD/ $\times 10^6 \text{ \AA}^{-2}$
Silicon	2.07
Silicon Oxide	3.49
Glue*	1.08
Mica	3.79
D ₂ O	6.30
H ₂ O	-0.56
Contrast matched water to silicon (CMSi)	2.07
C ₁₆ TAB	-0.26

Scattering length densities (SLD) of the materials and water contrasts used in this work are given in Table 1. Contrast matched waters were prepared by mixing D₂O and H₂O in appropriate ratios using an HPLC pump. Water described as contrast matched to silicon (here noted as CMSi) has the same scattering length density as silicon ($2.07 \times 10^{-6} \text{ \AA}^{-2}$) and was made from 38% D₂O and 62% H₂O by volume. The D₂O used in this study was provided by ISIS (Sigma Aldrich 99 %) and H₂O was from an ultrapure source (Millipore $18.2 \text{ M}\Omega \text{ cm}^{-1}$).

Specular neutron reflectivity measurements were made on the SURF reflectometer at ISIS, UK using time of flight mode. Measurements were made in the Q range 0.007 to 0.3 \AA^{-1} using three different grazing angles of incidence (0.25° , 0.6° , 1.5°). The neutron footprint, chosen as 35 mm x 75 mm to prevent clipping the edges of the Teflon trough, was held constant across all three angles using a series of collimating slits before the sample.

Data Analysis

A typical substrate for neutron reflection is considered as a series of layers. The Abeles matrix method is commonly used to calculate the reflected intensity arising from the system as a whole¹⁸. The amplitudes of reflected waves are added across each interface modulated by a phase term dependent on the distance travelled through the layer. Here it is assumed that the interfaces are sufficiently close that there is no loss of coherence as the radiation passes across the layer from one interface to the next.

However, in mica substrate the mica and glue layers are rather thicker than those encountered in neutron reflectivity studies and so a thick film approach similar to that used by Zarbakhsh *et al* is employed¹⁹. Loss of coherence of the radiation as it passes from one interface to the next means that reflectivity from a single thick layer (R_{01}) arises from the summation of reflected intensities each dampened by an attenuation term which depends of the path length of the radiation through the layer (l) and the attenuation cross section (σ_{tot}) and number density of atoms in the layer (N) as shown by Eq 1.

$$R_{01} = R_0 + \frac{(1 - R_0)^2 R_1 e^{-2Nl\sigma_{tot}}}{1 - R_0 R_1 e^{-2Nl\sigma_{tot}}} \quad \text{Eq 1}$$

The attenuation of the neutron beam by mica and Loctite® 3301 glue has been measured as a function of wavelength (see supporting information) and attenuation cross section parameters for each extracted from the data. The attenuation of the beam as a function of neutron wavelength was best parameterized in parabolic form for the glue (Eq 2) whilst a linear dependence was found to be most appropriate for the mica (Eq 3).

$$N\sigma_{tot,glue} = a_{glue}\lambda^2 + b_{glue}\lambda + c_{glue} \quad \text{Eq 2}$$

$$a_{glue} = -0.137 \times 10^{-9} \text{\AA}^{-3}, b_{glue} = 7.105 \times 10^{-9} \text{\AA}^{-2}, c_{glue} = 11.01 \times 10^{-9} \text{\AA}^{-1}$$

$$N\sigma_{tot,mica} = b_{mica}\lambda + c_{mica} \quad \text{Eq 3}$$

$$b_{mica} = 0.8738 \times 10^{-9} \text{\AA}^{-2}, c_{mica} = -0.1734 \times 10^{-9} \text{\AA}^{-1}$$

The path length through the layer is related to the angle of entry into the layer (θ_1) and the layer thickness (d_1) via Eq 4. Entry angle in the layer depends on the angle of incidence (θ_0) and the wavelength dependent refractive indices of the incident phase and the layer (n_0 and n_1 respectively).

$$l = \frac{d_1}{\sin\theta_1} \quad \text{Eq 4}$$

Existing reflectivity analysis packages are unsuitable for use in systems with thick layers. I-CALC, a fitting routine specifically programmed for calculating reflectivity from mica substrates, has been used to analyse the data using a combination of thick and thin film formalisms⁷.

Experimental data was collected at three separate angles in order to cover the full Q range. During the data reduction procedure, the full reflectivity profile is generated by combining data collected at three incident beam angles. Scaling of the data recorded at the middle angle to the highest angle, then scaling the data recorded at the smallest angle to the composition of the later two angles in the stitching process was used.

In analysis of reflectivity data from thin films, knowledge only of the momentum transfer to the surface (Q) is required because no path length dependent absorption terms are required. In analysis of reflectivity data from thick absorbing films, the angle of incidence is crucial in determining the correct form of the reflectivity as a function of Q . The wavelength dependence of the absorption cross section and path length through the layer cause an incident angle dependence on the form of the reflectivity as a function of Q . By contrast to reflection from thin films, we do not expect the reflected intensity to be continuous in Q with a change in the incident

angle. Nevertheless, based on model calculations, we expect that this discontinuity is indeed small and so usual data reduction routines can still be applied.

Reflectivity profiles calculated using the I-CALC program are generated for the three separate angles of incidence and a stitching procedure applied to generate the full the full profile in exactly the same way as the experimental data. Instrumental and sample related resolution smearing is included by convolution of the calculated reflectivity profile with full width half maximum related to the resolution $\frac{\Delta Q}{Q}$: here fitted to 7%.

Results and Discussion

Bare Mica Surface

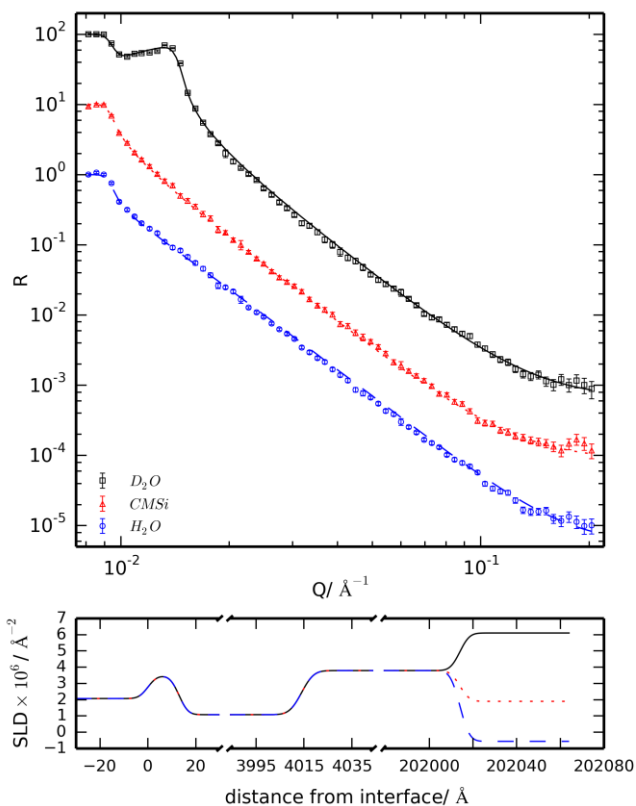


Figure 2 [top] Observed (points) and calculated reflectivity profiles of the bare surface in D₂O (squares), contrast matched to silicon water (CMSi- triangles) and H₂O (circles). Fitted lines are calculated for the bare surface according to a three layer model using the parameters given in Table 2. Data has been scaled such that the reflected intensity is unity prior to the first critical edge and D₂O and H₂O data sets are offset for clarity. [bottom] SLD profiles extracted from fits. The horizontal axis is split for clarity at interfaces of interest.

Table 2 Parameters used for fitting of the bare surface reflectivity profiles

Layer	Thickness	Roughness/ Å
Silicon Substrate	-	3 ± 2
Silicon Oxide	13 ± 2 Å	3 ± 2
Glue	0.4 ± 0.1 μm	4 ± 3
Mica	19.8 ± 0.5 μm	4 ± 2

Figure 2 shows the experimental reflectivity profiles collected from the bare mica/water interface against a subphase in three water contrasts: D₂O, CMSi and H₂O. Data collected in D₂O has two critical edges a feature which confirms that reflection is taking place from the mica/water interface. The condition for a critical edge is that the incident beam meets an interface where the SLD is higher across the interface from the incident beam. Here this criterion is met by both the mica layer and D₂O. Usually all reflected signal would be unity below the highest critical angle. However, here the beam attenuation by the mica reduces the scattering between the two critical edges meaning both are visible.

All data in Figure 2 was fitted using the same structural model with only the SLD of the subphase allowed to vary. The shift in position of the D₂O mica critical edge suggests that there was a small variation in the SLD of the subphase ($0.2 \times 10^{-6} \text{ \AA}^{-2}$) due to incomplete cell exchange (approximately 2% by volume). Hence the SLD of the subphase was permitted to vary slightly during the fitting procedure. The experimentally determined layer thicknesses and roughnesses are given in Table 2. The intensity of the data below the silicon/mica critical edge ($Q = 0.008$) in Figure 2 is scaled to unity.

The thicknesses of the glue and mica layers is relatively large and cannot be readily determined from the usual profile fitting but can be estimated from the beam attenuation and reduction in intensity between the two critical edges for mica⁷. In this work the thickness and structural characterisation of the adsorbed surfactant is of primary interest and this is not significantly affected by these glue and mica thicknesses.

Adsorption of C₁₆TAB Surfactant

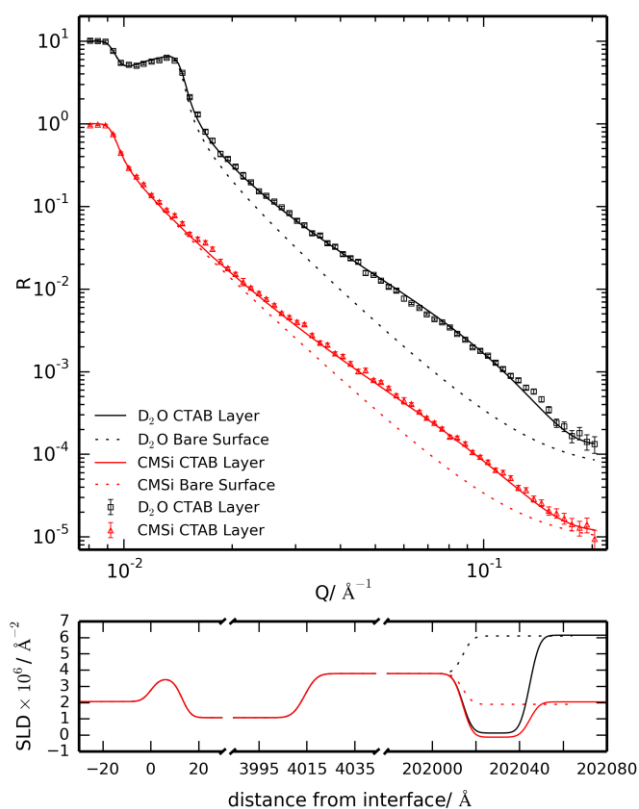


Figure 3 [top] Measured reflectivity profiles and fits to data plotted on a log-log scale. Fits for the bare surface are shown for comparison as dashed lines. D₂O contrasts are shown as squares and contrast matched to silicon (CMSi) contrasts as triangles. D₂O data and fit have been offset by a factor of ten for clarity. [bottom] SLD profiles extracted from fits.

Figure 3 shows the neutron reflection data for the mica surface with adsorbed C₁₆TAB at the CMC, 1.0 mM, in D₂O and CMSi and fits to the data from the bare surface for reference. Both contrasts show a large change relative to the bare surface; clear evidence that a surfactant layer has been adsorbed at the mica/water interface. The reflectivity profile for the surface exposed to C₁₆TAB in an H-contrast was not measured as there is

insufficient contrast between the subphase and surfactant. Both the D₂O and CMSi C₁₆TAB data sets were fitted simultaneously by adding single layer of constant SLD. Only roughness, thickness and SLD of the layer were allowed to vary whilst other structural parameters were kept constant at the values determined from characterisation of the bare surface. It was found that the data fitted well to this simple one layer model. Figure 4 presents a schematic illustration of the proposed surface structure of the system. A more complex three layer model for the bilayer consisting of inner surfactant head group, hydrocarbon tails outer head groups was also considered but the addition of these extra parameters showed no significant improvement on the quality of the fit so was not explored further.

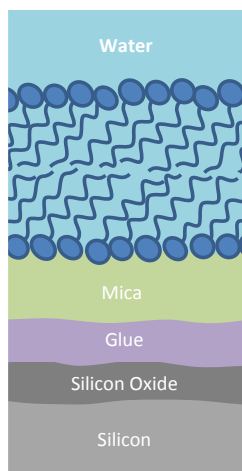


Figure 4 Schematic of the layer structure of mica supported on a silicon substrate with the C₁₆TAB adsorbate at with water mica interface. Not to scale.

The C₁₆TAB adsorbate was fitted to a single layer of thickness $31 \pm 1 \text{ \AA}$ with a roughness at the bilayer/water interface of $3 \pm 1 \text{ \AA}$ and layer hydration of $6 \pm 2 \%$. This adsorbed layer thickness is significantly smaller than twice the extended surfactant chain length (43.4 \AA calculated using Tanford's formula²⁰) suggesting significant tilting (44° to the surface normal) or

interdigitation of the hydrocarbon chains as shown in Figure 4. Based on this analysis we conclude that the C₁₆TAB structure at the mica/water interface is an essentially complete bilayer. Speranza *et al* measured the thickness of the C₁₆TAB layer as 30.1 Å with a roughness of 0.5 Å and 100% coverage with XRR. The C₁₆TAB bilayer thickness was measured as 31 to 36 Å by Kekicheff *et al* and Pashley *et al* using SFA⁸⁻¹⁰. Our measured values of thickness and roughness values are also in good agreement with these other experimental measurements providing further support that the surface self-assembled structure is, indeed, a bilayer.

A number of models for cylindrical or spherical micelles have also been considered in light of the micellar structures imaged with AFM observed in the first 6 - 24 h after initial adsorption. In the long time limit the AFM measurements also report adsorbed bilayers, as we report. It is only in the initial phase that periodic cylindrical micellar structures are indicated by AFM. In making our comparison we need to estimate the depth of the micelles normal to the surface, as these are not available from the AFM data. Here we have assumed it is reasonable to consider a micellar structure which will have layer thicknesses of approximately twice the extended molecular length. In calculating the reflectivity, these structures have been modelled here using 21 layers with varying layer hydration to capture to variation in solvent content for these surfactant morphologies.

Observations of C₁₆TAB on mica imaged using AFM by Ducker and Wanless indicate a micellar cylinders with a repeat spacing of 70 Å, noted to be significantly larger than twice the extended surfactant chain length (43.4 Å)¹⁴. They suggest a water gap and/or flattening of the micelles to explain this feature of their data; this water gap therefore, may be up to 26.6 Å, between the adsorbed cylinders.

Figure 5 presents the calculated reflectivity based on adsorbed compressed cylinders separated on the surface by a water gap of 15 Å (as an estimate of the structure put forward by Ducker and Wanless). (The calculated reflectivity expected from spherical micelles is also included in Figure 5) It is clear from Figure 5 that these calculated reflectivity profiles from the adsorbed micellar phases are distinct from the experimentally observed data and from the fitted bilayer.

The fitted neutron reflection data strongly indicates rather low amounts of water in the surfactant layer. Hence the agreement of the scattering with a complete bilayer, rather than the adsorbed micelles outlined above. We can find better agreement with our data in the limit of close packed very distorted ('flattened') cylinders with no hydration between adjacent head groups to minimize solvent inclusion in the layer. However, we consider this model to be somewhat unphysical since there would be strong electrostatic repulsion between the charged head groups. Hence we conclude that the adsorbed C₁₆TAB structure is an essentially complete bilayer.

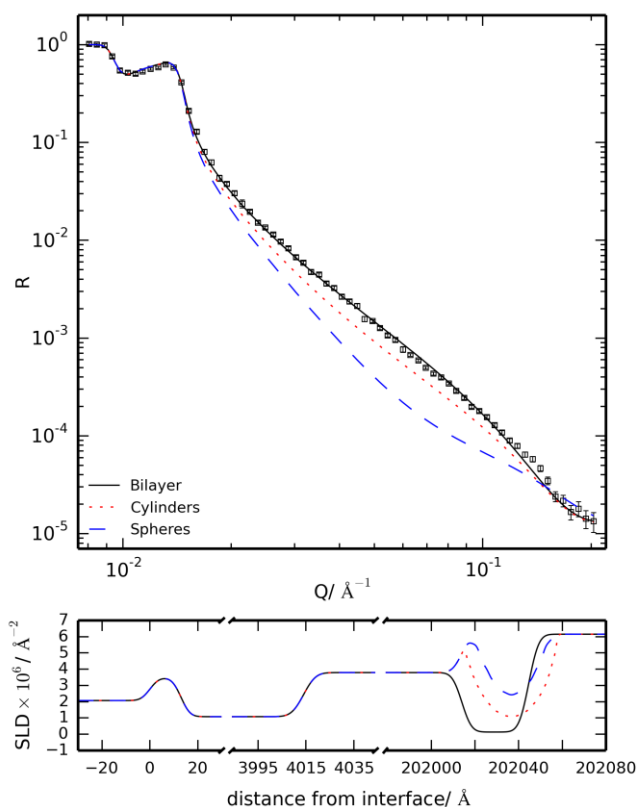


Figure 5 [top] Data collected for the bare surface and $C_{16}\text{TAB}$ layer at 1 CMC in D_2O along with fits to the data attempted using models for a bilayer, cylindrical micelles and spherical micelles. [bottom] SLD profiles extracted from fits.

Conclusions

We have shown that neutron reflection can be applied to the mica/water interface. The adsorbed structure of the $C_{16}\text{TAB}$ was determined to be an essentially complete bilayer using NR, a conclusion in good agreement with data from XRR, SFA and long time limit AFM studies. However, the data was not consistent with adsorbed micellar surface morphologies imaged using AFM when first deposited. It is suggested that the micellar surface morphologies may be induced

by the rapid lateral movements of the AFM tip where perturbation of the adsorbate provides a means of surfactant rearrangement on the surface.

Acknowledgements

We wish to thank ISIS (RB 1320050) for the allocation of beamtime and the beamline scientists for their assistance during the experiments. Manufacture and design of sample cells and technical help would not have been possible without the help of Andy Church (ISIS Sample environment), Andy Pluck (BP Institute), Sean Peacock and Alasdair Ross (University of Cambridge engineering department). We also thank our industrial sponsors, BP, and colleagues, Pete Salino and Isabella Stocker, for supporting this work (L. R. Griffin, K. L. Browning, C. L. Truscott and S. M. Clarke).

Supporting Information Available

Details on the parameterization of the wavelength dependence of neutron transmission through the glue and mica layers are presented in the supplementary information. This material is available free of charge via the Internet at <http://pubs.acs.org>.

Corresponding Author

* Stuart Clarke: stuart@bpi.cam.ac.uk

BP Institute and Department of Chemistry, University of Cambridge, Cambridge, CB3 0EZ

Funding Sources

BP RG63491

References

- (1) Fragneto, G.; Thomas, R. K.; Rennie, A. R.; Penfold, J. Neutron Reflection from Hexadecyltrimethylammonium Bromide Adsorbed on Smooth and Rough Silicon Surfaces. *Langmuir* **1996**, *12*, 6036–6043.
- (2) Rennie, A. R.; Lee, E. M.; Simister, E. A.; Thomas, R. K. Structure of a Cationic Surfactant Layer at the Silica-Water Interface. *Langmuir* **1990**, *6*, 1031–1034.
- (3) Penfold, J.; Tucker, I.; Petkov, J.; Thomas, R. K. Surfactant Adsorption onto Cellulose Surfaces. *Langmuir* **2007**, *23*, 8357–8364.
- (4) Schulz, J.; Warr, G.; Butler, P.; Hamilton, W. A. Adsorbed Layer Structure of Cationic Surfactants on Quartz. *Phys. Rev. E* **2001**, *63*, 041604–1 – 041604–041605.
- (5) McDermott, D. C.; McCarny, J.; Thomas, R. K.; Rennie, A. R. Study of an Adsorbed Layer of Hexadecyltrimethylammonium Bromide Using the Technique of Neutron Reflection. *J. Colloid Interface Sci.* **1994**, *162*, 304–310.
- (6) Cosgrove, T.; Heath, T. G.; Phipps, J. S.; Richardson, R. M. Neutron Reflectivity Studies of Polymers Adsorbed on Mica from Solution. *Macromolecules* **1991**, *24*, 94–98.
- (7) Browning, K. L.; Griffin, L. R.; Gutfreund, P.; Barker, R. D.; Clifton, L. A.; Hughes, A.; Clarke, S. M. Specular Neutron Reflection at the Mica Water Interface. *J. Appl. Crystallogr.* **2014**, *47*, 1638–1646.
- (8) Kekicheff, P.; Christenson, H. K.; Ninham, B. . W. Adsorption of Cetyltrimethylammonium Bromide to Mica Surfaces below the Critical Micellar Concentration. *Colloids and Surfaces* **1989**, *40*, 31–41.
- (9) Pashley, R. . Forces between Bilayers of Cetyltrimethylammonium Bromide in Micellar Solutions. *J. Colloid Interface Sci.* **1988**, *126*, 569–578.
- (10) Pashley, R. M.; Israelachvili, J. N. A Comparison of Surface Forces and Interfacial Properties of Mica in Purified Surfactant Solutions. *Colloids and Surfaces* **1981**, *2*, 169–187.
- (11) Chen, Y. L.; Chen, S.; Frank, C.; Israelachvili, J. Molecular Mechanisms and Kinetics during the Self-Assembly of Surfactant Layers. *J. Colloid Interface Sci.* **1992**, *153*, 244–265.
- (12) Lamont, R. E.; Ducker, W. A. Surface-Induced Transformations for Surfactant Aggregates. *J. Am. Chem. Soc.* **1998**, *120*, 7602–7607.

- (13) Liu, J.-F.; Ducker, W. A. Surface-Induced Phase Behavior of Alkyltrimethylammonium Bromide Surfactants Adsorbed to Mica, Silica, and Graphite. *J. Phys. Chem. B* **1999**, *103*, 8558–8567.
- (14) Ducker, W. a.; Wanless, E. J. Surface-Aggregate Shape Transformation. *Langmuir* **1996**, *12*, 5915–5920.
- (15) Briscoe, W. H.; Speranza, F.; Li, P.; Konovalov, O.; Bouchenoire, L.; van Stam, J.; Klein, J.; Jacobs, R. M. J.; Thomas, R. K. Synchrotron XRR Study of Soft Nanofilms at the Mica–Water Interface. *Soft Matter* **2012**, *8*, 5055.
- (16) Speranza, F.; Pilkington, G. A.; Dane, T. G.; Cresswell, P. T.; Li, P.; Jacobs, R. M. J.; Arnold, T.; Bouchenoire, L.; Thomas, R. K.; Briscoe, W. H. Quiescent Bilayers at the Mica–Water Interface. *Soft Matter* **2013**, *9*, 7028–7041.
- (17) Rosen, M. J. *Surfactants and Interfacial Phenomena*; John Wiley & Sons, 2004.
- (18) Heavens, O. S. *Optical Properties of Thin Solid Films*; Dover Publications, 1955; pp. 43–80.
- (19) Zarbakhsh, A.; Querol, A.; Bowers, J.; Webster, J. R. P. Structural Studies of Amphiphiles Adsorbed at Liquid-Liquid Interfaces Using Neutron Reflectometry. *Faraday Discuss.* **2005**, *129*, 155–167.
- (20) Tanford, C. Micelle Shape and Size. *J. Phys. Chem.* **1972**, *76*, 3020–3024.

Graphical Abstract + Synopsis

In this work we present neutron reflection data from an alkylammonium surfactant ($C_{16}TAB$) at the mica/water interface. The system is studied in situ in a non-invasive manner and indicates the formation of a complete adsorbed bilayer with little evidence of defects. A detailed analysis suggests that the data is not consistent with some other previously reported adsorbed structures, such as micelles or cylinders.

